Liquid Crystals
Publication details, including instructions for authors and subscription information:
http://www.informaworld.com/smpp/title~content=t713926090

An *Ia*3¯*d* thermotropic cubic phase from *N*-alkylpyridinium tetrahalocuprates

Francesco Neve[a]; Marianne Impéror-Clerc Corresponding author[b]
[a] Dipartimento di Chimica, Università della Calabria, I-87030 Arcavacata di Rende (CS), Italy [b] Laboratoire de Physique des Solides, UMR 8502, Bat 510 Université Paris-Sud, F-91405 Orsay Cedex, France

Online publication date: 25 May 2010

To cite this Article Neve, Francesco and Impéror-Clerc Corresponding author, Marianne(2004) 'An *Ia*3¯*d* thermotropic cubic phase from *N*-alkylpyridinium tetrahalocuprates', Liquid Crystals, 31: 7, 907 — 912
To link to this Article: DOI: 10.1080/02678290410001713351
URL: http://dx.doi.org/10.1080/02678290410001713351

Liquid Crystals, Vol. 31, No. 7, July 2004, 907–912

An $Ia\bar{3}d$ thermotropic cubic phase from *N*-alkylpyridinium tetrahalocuprates

FRANCESCO NEVE

Dipartimento di Chimica, Università della Calabria, I-87030 Arcavacata di Rende (CS), Italy

and MARIANNE IMPÉROR-CLERC*

Laboratoire de Physique des Solides, UMR 8502, Bat 510 Université Paris-Sud, F-91405 Orsay Cedex, France

(*Received 1 December 2003; in final form 10 March 2004; accepted 14 March 2004*)

The thermotropic liquid crystalline behaviour of two *N*-alkylpyridinium tetrahalocuprates was investigated. The *n*-pentadecyl tetrachloro and tetrabromo derivatives (CU15-CL and CU15-BR, respectively) exhibit very similar behaviour on cooling, and specifically, a high temperature smectic phase followed by a cubic phase. We fully elucidated the $Ia\bar{3}d$ space group for the cubic phase from X-ray diffraction on single crystals. The type of cubic phase is still under discussion, but we suggest that it is a direct type of structure based on the known phase sequence of lower and higher homologues. A model for the local organization of CU15-CL and CU15-BR in the cubic and smectic mesophases is also proposed.

1. Introduction

Supramolecular self-association of amphiphiles (i.e. molecules containing two incompatible — usually hydrophilic and hydrophobic — molecular components) is known to be a very important process both in life sciences and in materials science [1–5]. Self-assembled structures include spherical, columnar, lamellar, perforated lamellar and bicontinuous topologies, which may be rationalized in terms of the volume ratio of the hydrophilic (polar) to the hydrophobic (apolar) component within the structure. This model holds not only for crystalline solids [6] but also for block copolymers and liquid crystals (LCs) [7, 8]. Among the latter, lyotropic (i.e. solvent-driven) liquid crystals display the whole range of these topologies, giving rise to micellar, columnar, lamellar and cubic mesophases according to the hydrophobic/hydrophilic volume ratio and the interfacial curvature†.

*Author for correspondence; e-mail: imperor@lps.u-psud.fr

†The curvature argument is actually invoked to explain the local phase structure, with LC mean curvature values ranging from either positive or zero ('normal', 'direct' or Type I phases) to negative ('inverse', 'reversed' or Type II phases). In water–amphiphile systems, direct phases arise from the so-called oil-in-water situation. In solventless LC phases, interfaces are ideal surfaces separating polar regions from apolar ones. A more thorough discussion on direct and inverse phases, and a precise definition of interfacial curvature have been given by Seddon *et al.* [9].

Depending on their periodic structure, lyotropic mesophases with cubic symmetry can be divided into two groups. The first group covers micellar aggregates packed on a 3D lattice with possible space groups $Im\bar{3}m$, $Fm\bar{3}m$, $Pm\bar{3}n$, $Fd\bar{3}m$ (and even the $P6_3/mmc$ 3D-hexagonal space group [10]). The second and more fascinating group refers to bicontinuous phases [11]. In water–amphiphile binary systems, an inverse bicontinuous phase consists of an infinite bilayer of amphiphiles separating the space in two equivalent subspaces filled with water [12]. This bilayer has a curvature and is 3D-periodic. The direct topology also exists, where a water film separates two equivalent 3D-networks of rods made of the amphiphiles. In either case, common space groups of bicontinuous LC phases are $Ia\bar{3}d$, $Im\bar{3}m$, and $Pn\bar{3}m$.

Thermotropic (i.e. temperature-driven) and lyotropic LCs exhibit cubic mesophases with similar symmetry [13], yet thermotropic cubic phases have been far less extensively studied, although over the last decade this topic has received particular attention leading to an ever increasing activity in the area [8, 14, 15].

As part of our studies on self-assembling ionic mesogens [16], we have recently reported a homologous series of organic–inorganic compounds based on *N*-alkylpyridinium surfactants and $[CuCl_4]^{2-}$ inorganic anions in a 2:1 molar ratio [17]. These exhibit either columnar or lamellar thermotropic mesomorphism

Liquid Crystals ISSN 0267-8292 print/ISSN 1366-5855 online © 2004 Taylor & Francis Ltd
http://www.tandf.co.uk/journals
DOI: 10.1080/02678290410001713351

depending on the alkyl chain length of the cation, with lamellar order prevailing at longer chain lengths. Along the series (C_9 through C_{18}), only the C_{15} compound (CU15-CL) shows differing behaviour, by exhibiting an enantiotropic cubic phase that transforms into a smectic phase at higher temperature. The cubic phase of CU15-CL was characterized by polarizing optical microscopy (POM) and X-ray powder diffraction (XRPD), but no definitive assignment of the space group could be made [17].

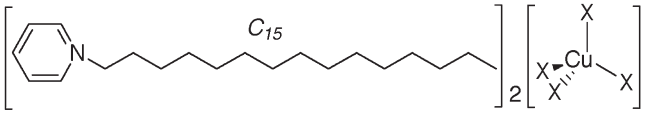

Cu15-X

In order to investigate this unusual behaviour in this class of ionic compounds, and to make an unambiguous assignment of the cubic phase structure, we have prepared CU15-Br (the bromine analogue of CU15-CL). In this paper, we show that both compounds exibit the same cubic phase, using diffraction experiments performed on single crystal samples. We discuss the structure of this cubic phase taking into account also the thermotropic behaviour of the other members of the Cu-*n*-*X* series (X = Cl, n = 12–18).

2. Results

The new compound CU15-BR was obtained as a blue–violet microcrystalline solid that exhibited an interesting phase sequence, figure 1 (*a*). On heating, at 64°C CU15-BR melted to an optically isotropic viscous phase. Since the melt was very dark, only an increase in fluidity indicated the subsequent transition to an isotropic liquid. On cooling the liquid phase, a well formed fan-shaped texture characteristic of a smectic phase soon appeared when viewed under crossed polarizers. The optically isotropic phase was then observed to develop as dark areas with straight edges on further cooling, figure 1 (*b*). Slow crystallization followed thereupon.

Optical observations were complemented by calorimetric and XRD measurements. Differential scanning calorimetry (DSC) confirmed the existence of two LC phases in the phase diagram of CU15-BR: an enantiotropic cubic phase and a metastable smectic phase. On heating, the crystal–cubic transition has a large associated enthalpy change ($\Delta H = 79.4\,\mathrm{kJ\,mol^{-1}}$), while clearing, observed at 81°C, occurs with a very small associated ΔH ($0.4\,\mathrm{kJ\,mol^{-1}}$). In the reverse cooling cycle, both the isotropic–smectic and smectic–cubic phase transitions have small negative ΔH values (0.1 and $0.2\,\mathrm{kJ\,mol^{-1}}$, respectively). Subsequent heating–cooling cycles confirmed the phase sequence observed during the first DSC run.

DSC results were substantiated by XRD. The two compounds CU15-CL and CU15-BR were observed both on heating and cooling at a relatively high rate of $12^\circ\mathrm{C\,min^{-1}}$ in order to avoid thermal decomposition of the samples. CU15-CL was heated only within the SmA phase region, while CU15-BR was heated for only 5 min within the isotropic liquid phase. The exposure times were 5 min, using a CCD camera detector and a high brilliance, synchrotron source. The results are summarized in table 1. The two compounds exhibit a high temperature SmA phase (only on cooling for CU15-BR), with layer thicknesses of 31.4 and 32.8 Å for CU15-CL and CU15-Br, respectively. On cooling from the smectic phase, the cubic phase grows in large monodomains, and single crystal diffraction patterns were recorded (figure 2). This observation was expected at the smectic to cubic phase transition as studied, for example, for the lyotropic $C_{12}E0_6/H_2O$ system [18]. From these patterns, the space group assignment is straightforward and the $Ia\bar{3}d$ space group is assigned unambiguously. A detailed

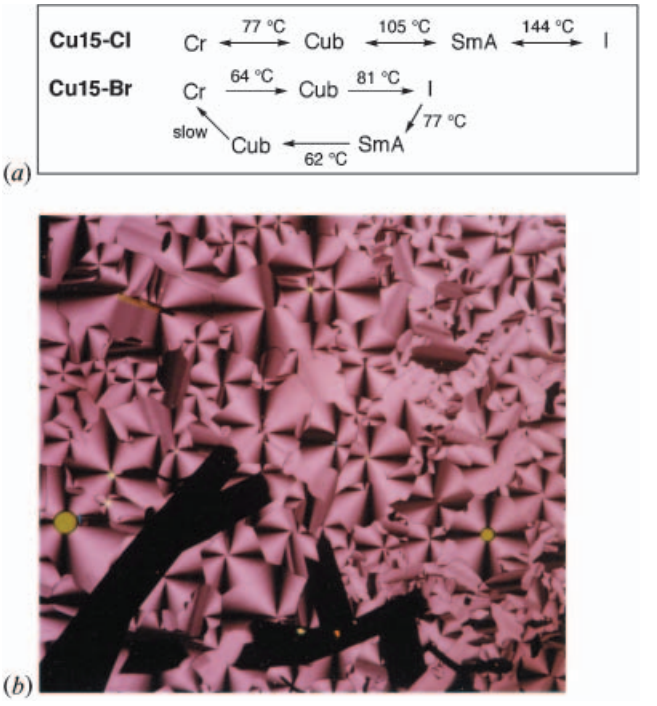

Figure 1. (*a*) Phase sequence for CU15-CL (see [17]) and CU15-BR. Cr = crystalline phase; Cub = cubic phase; Sm = smectic phase; I = isotropic liquid. (*b*) Optical polarizing micrograph (100×) of the cubic phase nucleation for CU15-BR on cooling from the smectic A phase at 62°C.

Table 1. X-ray diffraction data for CU15-CL and CU15-BR in the cubic phase and in the smectic A phase[a].

Phase		CU15-CL		CU15-BR	
$Ia\bar{3}d$ cubic phase		$T=85°C$ $a=80.5$ Å		$T=58°C$ $a=82.8$ Å	
$\{h\,k\,l\}$ indices	$h^2+k^2+l^2$	d (meas.) Å	d (calc.) Å	d (meas.) Å	d (calc.) Å
2 1 1	6	32.9	32.9	33.6	33.8
2 2 0	8	28.6	28.5	29.5	29.3
3 2 1	14	21.4	21.5	21.9	22.1
4 0 0	16	—	20.1	—	20.7
4 2 0	20	—	18.0	18.5	18.5
3 3 2	22	—	17.2	17.6	17.7
4 2 2	24	16.4	16.4	—	16.9
4 3 1	26	—	15.8	16.4	16.2
SmA phase		$T=130°C$ d (meas.) Å 31.4		$T=75°C$ d (meas.) Å 32.8	

[a]a is the unit cell parameter of the cubic lattice. d (meas.) and d (calc.) are the observed and calculated d-spacings of the small angle $\{h\,k\,l\}$ reflections.

indexing of the patterns is given in figures 3 and 4. The two strongest $h\,k\,l$ reflections are of the type (2 1 1) and (2 2 0), and are the first reflections permitted by the space group. Furthermore, characteristic diffuse scattering lines are observed between these, as for other systems, revealing the same cubic phase [18]. The d-spacing values are given in table 1. The cubic lattice parameter a is 80.5 Å for CU15-CL and 82.8 Å for CU15-BR.

The structure of the $Ia\bar{3}d$ cubic phase has been described already in detail in the literature [12, 18–20]. It is a bicontinuous phase consisting of two 3D-networks of rods, connected three by three at each node of the networks. These two 3D-networks are separated by an infinite periodic minimal surface [21] called the Gyroid surface (see figure 5) in the case of the $Ia\bar{3}d$ space group [19, 22]‡. In figure 3 and 4 these two networks are drawn in red and blue with the orientation of the unit cell corresponding to the diffraction patterns obtained [23]. The inverse (polar groups on the networks) and direct (chains on the networks) topologies are *a priori* both possible and will be discussed next.

3. Discussion

By analogy with the general class of flexible amphiphiles [8], the behaviour of the Cu-n-X compounds should be governed mainly by the segregation of the n-alkyl chains and the polar groups. A critical parameter is the volume fraction occupied by each component. A large paraffinic volume fraction favours inverse phases while smaller volumes correspond to direct phases. Moreover, on increasing the paraffinic volume fraction, the following sequence of mesophases is predicted: direct micellar cubic, direct hexagonal, direct bicontinuous cubic, lamellar (equivalent term for SmA), inverse bicontinuous cubic, inverse hexagonal phase, inverse micellar phase.

Along the Cu-n-X series, on increasing the chain length n (i.e. the paraffinic volume fraction), one observes hexagonal phases for $n=12$ to 14, a lamellar phase for $n=15$ to 18, and the cubic phase only for $n=15$. This phase sequence is in accord with hexagonal and cubic phases of the direct type. However, in the absence of a direct knowledge of the molecular volumes (unfortunately we were unable to perform dilatometry experiments) it is a difficult task to establish from our X-ray data whether the phases are direct or inverse. Here, following the predicted phase sequence, we argue that the cubic phase for the $n=15$ compounds is a direct phase, although an inverse phase cannot be ruled

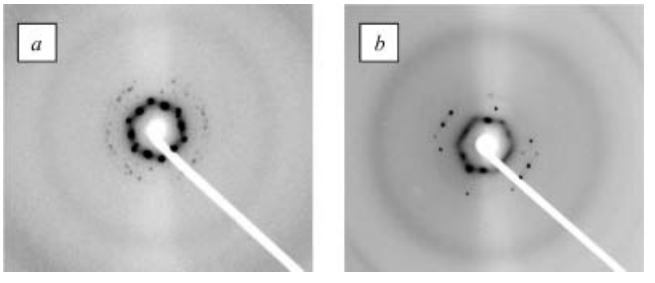

Figure 2. X-ray diffraction pattern of a cubic monodomain of (*a*) CU15-CL and (*b*) CU15-BR.

‡Triply periodic minimal surfaces (TPMS) are mathemathical models for bicontinuous cubic phases. A graphical representation of the simplest TPMS surfaces with cubic symmetry can be retrieved at the following URL: http://msri.org/publications/sgp/SGP/main.html. Sadoc and Charvolin have given a crystallographic description of TPMS [22].

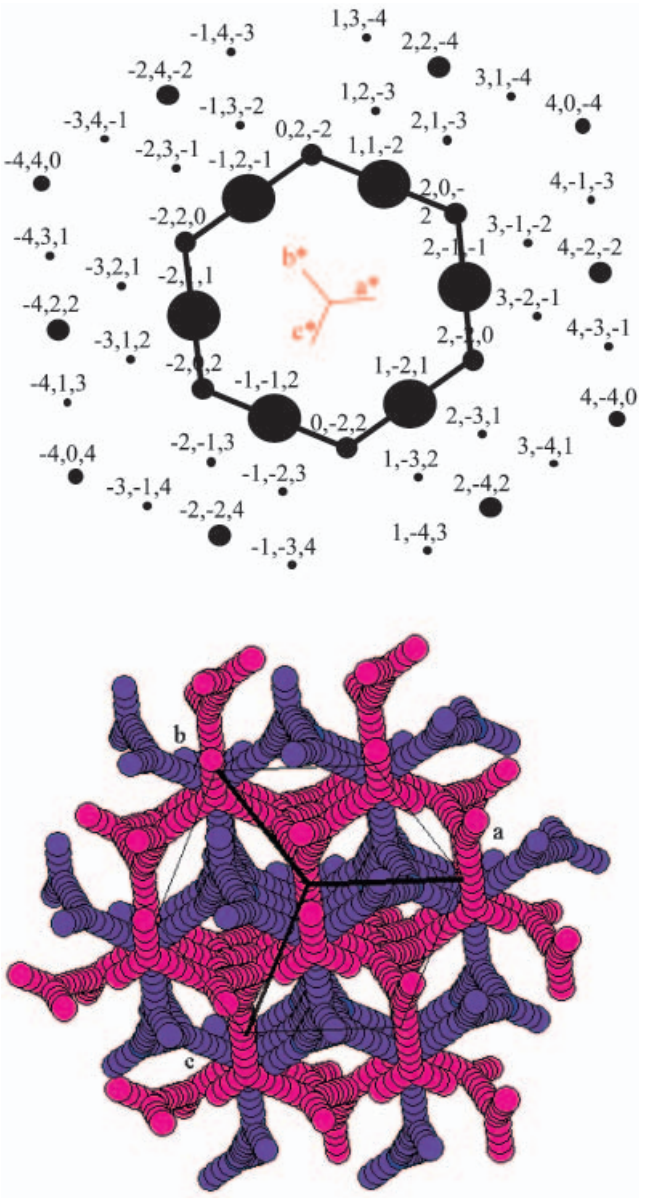

Figure 3. Indexing of the reciprocal plane of CU15-Cl and the corresponding orientation of the cubic monodomain in real space.

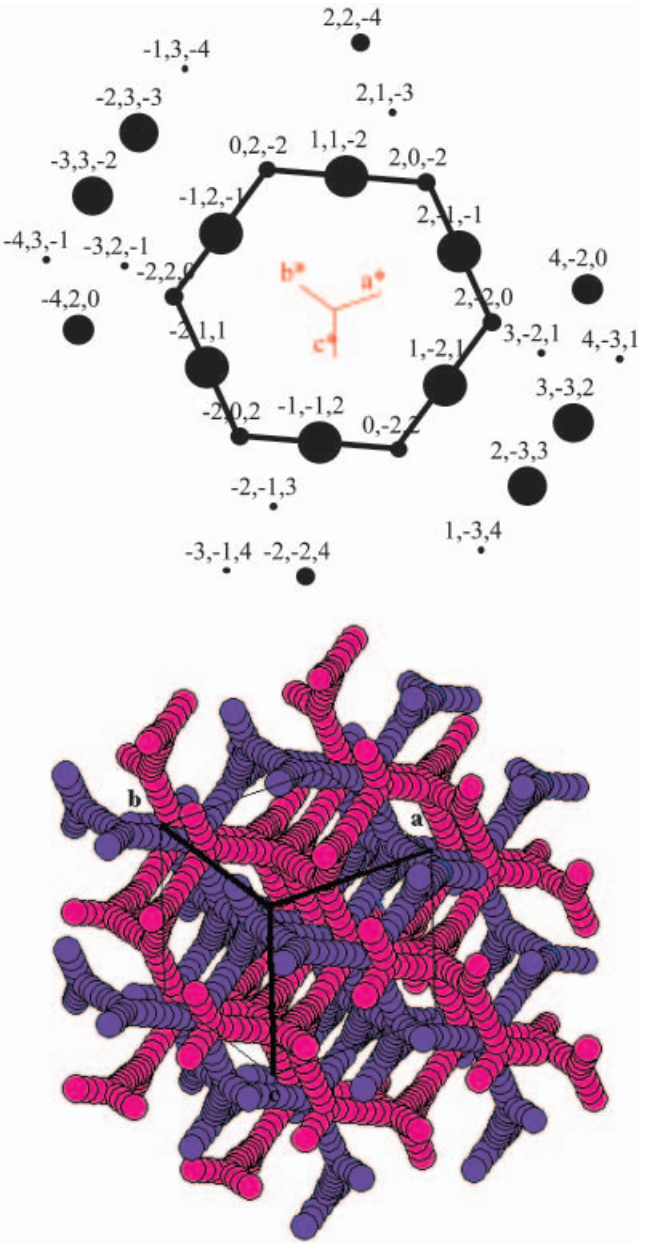

Figure 4. Indexing of the reciprocal plane of CU15-BR and the corresponding orientation of the cubic monodomain in real space.

out. As shown in figure 5, we assume that the polar groups (CuX_4^{2-} anions plus pyridinium cation headgroups) are located around the Gyroid surface, forming a film of average thickness L_{polar}. Each polar group occupies on average an area per anion, σ_{anion}, which is the ratio of the area of the Gyroid surface to the average number of anions inside one cubic unit cell. The alkyl chains are inside the two 3D-networks (in blue and red). Then, we estimate the molecular parameters inside the two mesophases of the $n=15$ compounds. Reasonable estimates of the paraffinic volume fraction (ϕ_{para}) give values between 0.55 and 0.7 for these compounds [24].§

§In the crystalline phase of CU15-CL, the total density equals $\rho_{tot}=1.13\,g\,cm^{-3}$, and the paraffinic volume fraction equals 0.67 with $\rho_{para}=0.9\,g\,cm^{-3}$ and $\rho_{polar}=1.61\,g\,cm^{-3}$. We make the following assumptions inside the mesophases: $0.7<\rho_{para}$ $(g\,cm^{-3})<0.8$ (by comparing with the known molten *n*-alkanes density in the temperature range of our study [24]); ρ_{polar} $(g\,cm^{-3})<1.61$; $2*1.13/3=0.75<\rho_{tot}$ $(g\,cm^{-3})<1.13$; $\rho_{para}<\rho_{polar}$.

Table 2. Molecular quantities for the two mesophases. The density of the alkyl chains ρ_{para} is assumed to be between 0.7 and 0.8 g cm^{-3} [24]. For CU15-Cl, the total density ρ_{tot} is taken between 0.8 and 1 g cm^{-3} and the average density of the polar groups ρ_{pol} between 1 and 1.5 g cm^{-3}. For CU15-Br, the total density ρ_{tot} is assumed between 1 and 1.2 g cm^{-3} and the average density of the polar groups ρ_{pol} between 1.3 and 2 g cm^{-3}.

Phase	CU15-CL or CU15-Br
$Ia\bar{3}d$ cubic phase	
a Å	80–83
N anions / cubic cell	340–440
σ/anion Å^2	50–60
ϕ_{para}	0.58–0.65
L_{polar} Å[a]	9–12
SmA phase	
d Å	30–33
σ/anion Å^2	40–50
ϕ_{para}	0.6–0.7
L_{polar} Å	10–13

[a]The average thickness L_{polar} of the polar region around the Gyroid surface (figure 5) is calculated solving the equation : $\phi_{para}\, a^3 = 2\,(\sigma_c\, a^2\, L_{polar} - 16\,\pi\, L_{polar}^3/3)$ where $\sigma_c = 3.091$ is a geometric parameter from the Gyroid surface [19].

In table 2, we give the resulting molecular parameters for the two mesophases, making additional hypotheses on the mesophase densities. This leads to a global description of both mesophases, with a flat polar film in the case of the smectic phase ($L_{polar} = 10$–13 Å, $\sigma_{anion} = 40$–50 Å^2) and a curved polar film for the direct cubic phase ($L_{polar} = 9$–12 Å, $\sigma_{anion} = 50$–60 Å^2). The thickness is in the same range for the two mesophases. The value of area per anion σ_{anion} is around 50 Å^2. This value is about twice the usual value for the molecular area of molten alkyl chains (23–25 Å^2). Since in the case of an ideal bilayer model one would find $\sigma_{anion} = \sigma_{chain}$, then here the alkyl chains are probably partially interdigitated (figure 5).

The phase behaviour of CU15-CL and CU15-BR requires one final comment. The richer polymorphism (and superior thermal stability of the mesophases) of CU15-CL is in perfect agreement with previous observations for analogous Pd(II) salts [25]. A key factor is related to the occurrence of extended C–H$\cdots X$–M H-bonding interactions in the condensed (and possibly liquid crystalline) state. In fact, the degree and strength of hydrogen bonding is expected to be very important in the crystalline (or highly ordered) phase of *N*-alkylpyridinium tetrahalometallates [17, 25–27]. With respect to tetrachlorometallates, general rules predict weaker C–H$\cdots X$–M bonds for bromo and iodo analogues. Thus, melting temperatures are expected to

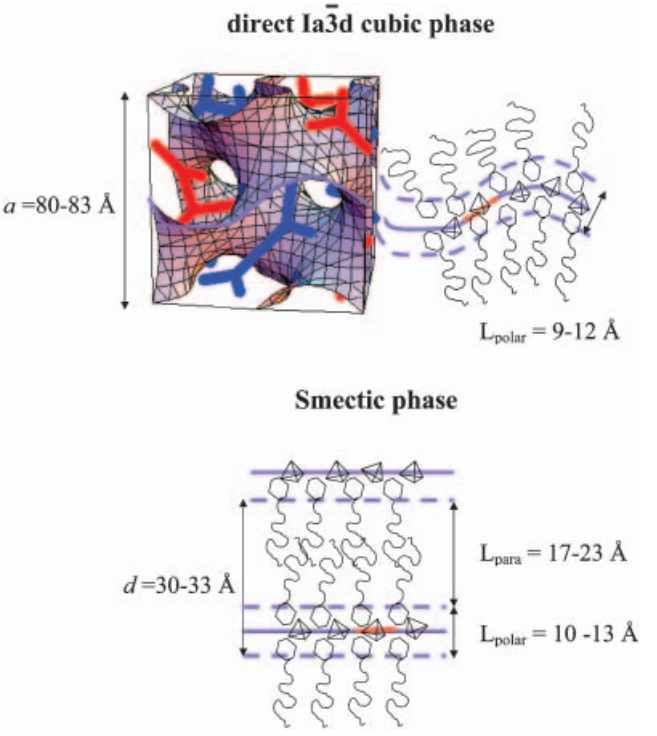

Figure 5. Proposed supramolecular structure for the $n = 15$ compounds. The polar groups form a film of average tickness L_{polar}, and average area per anion σ_{anion} (in red). In the case of the cubic phase, this film is assumed to be limited by two symmetrical surfaces (dotted lines) on both sides of the Gyroid surface (thick line).

follow the trend Cl > Br > I for a given chain length n value (at least if the solids are isomorphous). This has been observed along the series $[PdX_4]^{2-}$ *N*-alkylpyridinium derivatives [25, 26]. Clearing temperatures followed a less clearcut trend, suggesting that stabilization of the mesophase(s) in these ionic mesogens is due to multiple factors including H-bonding.

4. Conclusions

Thermotropic cubic phases are becoming increasingly observed [8, 14] both bicontinuous and micellar examples. Here we have reported an example of ionic thermotropic amphiphiles which exhibit a cubic phase in their phase sequences. We assigned the $Ia\bar{3}d$ space group to the cubic phase, which is described as a bicontinuous structure. As with cubic phases shown by lyotropic materials and block-copolymers, we discussed the direct or inverse nature of the cubic phase, suggesting a preference for a direct structure in the present case. It is therefore interesting to draw a parallel with the behaviour of potassium dialkylphosphate salts [20], a case where inverse structures are invoked. Those salts form an inverse $Ia\bar{3}d$ cubic phase and an inverse hexagonal phase on heating and also on

increasing the alkyl chains length. Thus, the phase sequence argument appears to hold and this might be a good way to assess the type of cubic phase. Finally, for the $Ia\bar{3}d$ thermotropic cubic phases already known, the inverse phase structure seems to dominate [14, 20]. At least one example of direct $Ia\bar{3}d$ cubic phase, however, can be found in the recent work of Skoulios *et al.* [28]. More interestingly, the cubic phase of alkylammonium poly(vinylsulfonate)s was described as consisting of curved molecular bilayers of amphiphiles [28]. Here, we suggest that the thermotropic mesomorphism of the Cu15-*X* compounds is well supported by assuming direct phases and a partially interdigitated bilayer-type model, a mesophase organization which is preserved across the smectic–cubic phase transition.

5. Experimental

Optical observations were made with a Zeiss Axioskop polarizing microscope equipped with a heating stage and a temperature control unit. DSC measurements were carried out with a Perkin-Elmer Pyris-1 instrument operating at a scanning rate of $5^{\circ}C\,min^{-1}$.

X-ray diffraction measurements were carried out at the LURE synchrotron facility (Orsay, France) at the D43 experimental station. A monochromatic beam (wavelength 0.1448 nm) was used using a Ge monochromator. The samples were introduced into Lindemann glass capillaries (diameter 1 mm) sealed at both ends. Capillaries were held inside a home-made oven. Detection was performed on a CCD camera (Princeton Instruments) at a distance of 77.3 mm from the sample. The software CaRine Crystallography 3.1 was used to visualize reciprocal and real lattices [23].

For the synthesis of CU15-BR, solid $CuBr_2$ (0.1 g, 0.45 mmol) was added to a colourless solution of *N*-pentadecylpyridinium bromide [25] (0.31 g, 0.90 mmol) in acetonitrile (10 ml), and immediately afforded a dark green–blue solution. The solution was heated at reflux for 30 min, and was then allowed to cool to room temperature. The product was recovered as blue needles, washed with diethyl ether and dried in air; yield 0.35 g (80%). Elemental analysis: calcd for $C_{40}H_{72}Br_4CuN_2$ (964.2) C 49.83, H 7.53, N 2.91; found C 49.83, H 7.50, N 3.38%.

References

[1] Ringsdorf, H., Schlarb, B., and Venzmer, J., 1988, *Angew. Chem. int. Ed. Engl.*, **27,** 113.

[2] Vögtle, F., 1991, *Supramolecular Chemistry* (New York: Wiley).

[3] Fuhrhop, J.-H., and Köning, J., 1994, *Membranes and Molecular Assemblies: the Synkinetic Approach* (Cambridge: The Royal Society of Chemistry).

[4] Lehn, J. M., 1995, *Supramolecular Chemistry: Concepts and Perspectives* (Weinheim: VCH).

[5] For recent reviews, see (*a*) Raimondi, M. E., and Seddon, J. M., 1999, *Liq. Cryst.*, **26**, 305; (*b*) van Bommel, K. J. C., Friggeri, A., and Shinkai, S., 2003, *Angew. Chem. int. Ed. Engl.*, **42**, 980; (*c*) Faul, C. F. J., and Antonietti, M., 2003, *Adv. Mater.*, **15**, 673.

[6] Xu, Z., Kiang, Y.-H., Lee, S., Lobkovsky, E. B., and Emmott, N., 2000, *J. Am. chem. Soc.*, **122,** 8376.

[7] Hamley, I. W., 1998, *The Physics of Block Copolymers* (Oxford: Oxford University Press).

[8] (*a*) Tschierske, C., 2001, *J. mater. Chem.*, **11**, 2647; (*b*) Tschierske, C., 2002, *Curr. Opin. colloid interface Sci.*, **7**, 355.

[9] Seddon, J. M., Robbins, J., Gulik-Krzywicki, T., and Delacroix, H., 2000, *Phys. Chem. chem. Phys.*, **2,** 4485.

[10] Clerc, M., 1996, *J. Phys. II Fr.*, **6,** 961.

[11] Scriven, L. E., 1976, *Nature*, **263,** 123.

[12] Charvolin, J., and Sadoc, J.-F., 1987, *J. Phys. (Fr.)*, **48,** 1559.

[13] Diele, S., and Göring, P., 1998, in *Handbook of Liquid Crystals*, edited by D. Demus, J. Goodby, G. W. Gray, H.-W. Spiess, and V. Vill, Vol. 2B, (Weinheim: Wiley-VCH), Chap. XIII.

[14] (*a*) Tschierske, C., 2002, *Curr. Opin. colloid interface Sci.*, **7**, 69; (*b*) Diele, S., 2002, *Curr. Opin. colloid interface Sci.*, **7**, 333; (*c*) Kutsumitzu, S., 2002, *Curr. Opin. solid state mater. Sci.*, **6**, 537.

[15] For recent examples, see: (*a*) Fazio, D., Mongin, C., Donnio, B., Galerne, Y., Guillon, D., and Bruce, D. W., 2001, *J. mater. Chem.*, **11**, 2852; (*b*) Imperor-Clerc, M., Veber, M., and Levelut, A.-M., 2001, *ChemPhysChem*, 533; (*c*) Fuchs, P., Tschierske, C., Raith, K., Das, K., and Diele, S., 2002, *Angew. Chem. int. Ed. Engl.*, **41**, 628.

[16] Neve, F., 1996, *Adv. Mater.*, **8,** 277.

[17] Neve, F., Francescangeli, O., Crispini, A., and Charmant, J., 2001, *Chem. Mater.*, **13,** 2032.

[18] Clerc, M., Levelut, A. M., and Sadoc, J.-F., 1991, *J. Phys. II Fr.*, **1,** 1263.

[19] Clerc, M., and Dubois-Violette, E., 1994, *J. Phys. II Fr.*, **4,** 275.

[20] Paleos, C. M., Kardassi, D., Tsiourvas, D., and Skoulios, A., 1998, *Liq. Cryst.*, **25,** 267.

[21] Schoen, A. H., 1970, Technical Note NASA TN D-5541; Schoen, A. H., 1969, *Nat. Am. Math. Soc.,* **16,** 519.

[22] Sadoc, J. F., and Charvolin, J., 1989, *Acta Crystallogr.*, **A45,** 10.

[23] Boudias, C., and Monceau, D., 1998, *CaRine Cristallography* version 3.1, http://perso.wanadoo.fr/carine.crystallography/.

[24] Reiss-Husson, F., and Luzzati, V., 1964, *J. Phys Chem*, **68,** 3504; Dee, G.T., Ougizawa, T., and Walsh, D. J., 1992, *Polymer*, **33**, 3462; Errington, J. R., and Panagiotopoulos, A. Z., 1999, *J. Phys Chem B*, **103**, 6314.

[25] Neve, F., Crispini, A., Armentano, S., and Francescangeli, O., 1998, *Chem. Mater.*, **10,** 1904.

[26] Neve, F., Crispini, A., and Francescangeli, O., 2000, *Inorg. Chem.*, **39,** 1187.

[27] Neve, F., Francescangeli, O., and Crispini, A., 2002, *Inorg. Chim. Acta*, **338,** 51.

[28] Tsiourvas, D., Paleos, C. M., and Skoulios, A., 1999, *Macromolecules*, **32,** 8059.